Carbohydrate Research, 221 (1991) 123–144
Elsevier Science Publishers B.V., Amsterdam

Solution conformation and dynamics of the octadeoxynucleotide d(CACTAGTG)$_2$: a multinuclear n.m.r. relaxation study

Andrew N. Lane
National Institute for Medical Research, The Ridgeway, Mill Hill, London NW7 1AA (Great Britain)

(Received February 27th, 1991; accepted for publication June 5th, 1991)

ABSTRACT

The conformation and internal dynamics of the octadeoxynucleotide d(CACTAGTG)$_2$ have been examined by ^{1}H- and ^{13}C-n.m.r. relaxation. All the non-exchangeable protons, the seven phosphate resonances, and most of the ^{13}C resonances of the proton-bearing carbons have been assigned by conventional two-dimensional n.m.r. methods. The average conformations of each nucleotide have been determined using time-dependent one-dimensional n.O.e.'s and $^3J_{HH}$ values derived from both NOESY and 2-quantum-filtered COSY experiments. All glycosidic torsion angles are anti, and in the range −95 to 125°, in which the pyrimidines have a significantly larger angle than the purines. All sugars were found mainly (>80%) in the conformation range C-2'endo to C-3'exo. The DNA fragment is within the B-family of conformations. The cytosine H-6–H-5 vectors move with an apparent correlation time of 3 ns at 25°. Cross-relaxation rate constants for the H-1'–H-2b vectors and some H-2a–H-2b and H-2a–H-3' vectors were measured, from which order parameters were determined. The order parameters are all in the range 0.7–0.9, which is consistent with only moderate internal mobility on the sub-ns time scale. The $\{^1H\}$–^{13}C n.O.e. and the spin–lattice relaxation rate constant show that the terminal residues are relatively more mobile than the internal residues, and that the C-2'–H and C-3'–H vectors move with order parameters of 0.6–0.75.

INTRODUCTION

In principle, the conformation of oligonucleotides in solution can be determined by high-resolution n.m.r. methods by making use of the dependence of the $^3J_{HH}$ values on the torsion angles, and the dependence of the n.O.e. on internuclear distances. For a rigid molecule in a unique conformation, conformational analysis is relatively straightforward, provided that there are sufficient independent data to determine the conformational parameters. Several methods of deriving the conformation from the *J* values and n.O.e.'s have been applied to oligonucleotides, with various degrees of success[1–12].

Generally, it has been assumed that there is a single conformation, when there is a simple relationship between n.O.e. and distance, provided that effects of spin-diffusion are properly accounted for[11–13]. The simple relationship between distance and n.O.e. intensity or, more correctly, the cross-relaxation rate constant, breaks down as soon as conformational averaging is present[14]. The low-amplitude, high-frequency motions of all atoms and groups of atoms that occur on the time-scale of ps have relatively small effects on the observable n.m.r. parameters[15,16]. However, motions having larger amplitudes due to interconversion among two or more distinct conformations can have large

0008-6215/91/$03.50

effects on the observable n.m.r. parameters, and the magnitude of these effects depends on the relative frequency of the interconversion[13,15–17]. One well-characterised source of conformational heterogeneity in mononucleosides is pseudorotation in the five-membered furanose ring. Because of the asymmetric substitution on the ring system, there are two main potential minima separated by ~2 kcal/mol, and which correspond roughly to the C-2′endo and C-3′endo states[18,19]. These states can be readily distinguished by measurements of the coupling constants[8,20,21]. However, the question as to whether the same potential function remains valid for a nucleotide embedded in a polymer remains controversial.

Altona and co-workers[8,20] have presented evidence that a conformational mixture of C-2′endo and C-3′endo states represents the best simple description of nucleotides in short oligomers (where enough coupling constants can be measured with sufficient accuracy). However, "end-effects" persist up to three base-pairs from each end of an oligomer[22], so it is not necessarily true for longer oligomers that such a description is more accurate than one in which a single, intermediate, conformation is postulated. For longer oligomers (*i.e.*, > 12 base pairs), where data are relatively scarce, there is a choice of how to describe sugar conformation. Although the alternative descriptions of the sugar pucker usually have little influence on the determination of the glycosidic torsion angle, they do have a substantial influence on the positioning of the phosphate backbone[16]. Several groups have therefore measured relaxation rates in order to determine whether the sugars are subject to conformational averaging[23–26].

The cross-relaxation rate constant for the H-2′a–H-2′b vector in $d(CGCGAATTCGCG)_2$[23] and in the hexamer $d(CGTACG)_2$[25] was identical with that expected for a vector moving with a correlation time equal to that of the cytosine H-6–H-5 vectors. The assumption that the bases do not undergo rapid internal motions was taken to imply that the sugars are also immobile on the ns time-scale. The bases undergo a rapid oscillation of amplitude of up to 20°[25–27], which is not experienced by the phosphates that are usually considered to be the most mobile groups in DNA[28,29]. Further, the H-1′–H-2′b vectors, which are perpendicular to the H-2′a–H-2′b vectors, appear more mobile than the Cyt H-6–H-5 vectors, which is consistent with rapid fluctuations about an axis parallel to H-2′a–H-2′b. This behaviour is not expected if rapid pseudorotation is the dominant motion[25], nor was there any correlation between the observed order parameters characterising the motions, and the mole fraction of the C-2′endo state. Further, Huang *et al.*[24] have measured the relaxation rates of a deuteron attached to C-2′ of the two adenosine residues in $d(CGCGAATTCGCG)_2$. Their results were inconsistent with a fluctuation between the C-2′endo and C-3′endo states, for mole fractions of C-2′endo (*i.e.*, f_s) < 0.9. However, according to Bax and Lerner[30], both of these residues are > 0.95 C-2′endo, so that no relaxation method will be sensitive to this kind of motion. The observed motion of the CD vector must therefore arise from some other motion, possibly the one responsible for the motion of the H-1′–H-2′b vector.

In order to address further the problem of internal motions in DNA, a multinuclear relaxation study of an octamer was undertaken. An octamer, the dimensions of which are approximately 27 × 23 Å, tumbles essentially isotropically, which simplifies

any analysis. Overall correlation times were determined from the Cyt H-6–H-5 vectors and from ^{13}C relaxation rate constants. Correlation times of any HH or CH vectors that are significantly smaller than the overall tumbling time must be ascribed to internal mobility of significant amplitude, on a time-scale of nanoseconds or faster.

EXPERIMENTAL

Materials. — The octanucleotide d(CACTAGTG) was synthesised by the phosphoramidite method (10 μmol) and purified by f.p.l.c. as described[25]. The oligomer was dissolved in water (0.5 mL) containing 10mM Na phosphate, 0.1M KCl, 0.1mM 2,2'-dimethylsilapentane-5-sulphonate (DSS), and 0.1mM EDTA (pH 7.0), and annealed by cooling the solution slowly from 80°. The annealed duplex was lyophilised and redissolved in 100% D_2O (0.6 mL).

Methods. — ^1H-N.m.r. spectra were recorded at 9.4 T and 25° on a Bruker AM400 spectrometer. One-dimensional truncated n.O.e. spectra were recorded using the method of Wagner and Wüthrich[31] with 16384 complex data points over a spectral width of 4 kHz. Typically, 400 free-induction decays were acquired per irradiation, and 2-Hz line broadening was used for processing difference spectra. Phase-sensitive two-dimensional spectra were obtained using the time-proportional phase-incrementation scheme[32]. Sine-modulated data were collected with appropriate adjustment of the receiver phase and optimisation of the dead-time to give a flat base plane[33]. The NOESY spectrum was acquired with 4096 points in F2 and 512 points in F1 over a spectral width of 4 kHz, with zero-filling to 8192 by 2048 complex points, giving a digital resolution of 0.97 Hz per point in F2. The data were apodised and resolution-enhanced with a 60°-shifted sine-squared bell in both dimensions before Fourier transformation. The two-quantum-filtered COSY spectrum was recorded also with 4096 points in F2 and 512 points in F1, over a spectral width of 4 kHz. Correlation times (τ) for the cytosine H-6–H-5 vectors were determined from the cross-relaxation rate constant (σ) derived from non-linear regression to the equation[34]:

$$\text{n.O.e.} = \sigma/\rho[1-\exp(-\rho t)], \quad (1)$$

$$\text{with } \sigma = 56.92/r^6[6J(2\omega)-J(0)], \quad (2)$$

and the spectral density functions

$$J(2\omega) = \tau/(1+4\omega^2\tau^2) \text{ and } J(0) = \tau, \quad (3)$$

where ω is the Larmor frequency.

Cross-relaxation rate constants for other vectors were obtained by non-linear regression to n.O.e. time courses as previously described[25]. Nucleotide conformations were derived from n.O.e. time courses for the H-8/H-6 to H-1', H-2'a, H-2'b, and H-3' spins, using the program NUCFIT[16].

^{13}C-N.m.r. spectra were recorded at 11.75 T and 25° on a Bruker AM500 spectrometer. The heteronuclear shift-correlation spectrum was recorded using 4096 points in F2 over a spectral width of 29.4 kHz, and 144 points in F1 over a spectral width

of 4 kHz. The data matrix was zero-filled to 4096 by 512 points and the free-induction decays were apodised with 5-Hz line broadening before Fourier transformation. Spin–lattice relaxation rate constants (R_1) were determined using FIRFT[35], and the heteronuclear n.O.e. using the gated decoupler experiments with a relaxation delay of 2 s. Relaxation rate constants were determined from the magnetisations by non-linear regression to the following equations:

$$M(t) = \mathrm{a} + \mathrm{bexp}(-R_1 t) \tag{4}$$

$$M(t) = M_0 \mathrm{exp}(-R_2 t) \tag{5}$$

where $M(t)$ is the magnetisation at time t, a and b are constants, and M_0 is the magnetisation at $t = 0$. Correlation times and order parameters for the CH vectors were determined from the relaxation rates according to the equation:

$$R_1 = 0.1\hbar^2\gamma_H^2\gamma_C^2[J(\omega_H - \omega_C) + 3J(\omega_H + \omega_C) + 6J(\omega_C)]. \tag{6}$$

Internal motions are treated using the formalism of Lipari and Szabo[36,37], for which the spectral density functions become:

$$J(\omega) = S^2 J(\omega, \tau_c) + (1 - S^2)J(\omega, \tau_e), \tag{7}$$

where S^2 is the generalised order parameter, τ_c is the correlation time for overall tumbling, and τ_e is a composite correlation time defined as:

$$\tau_e = \tau_c\tau_i/(\tau_c + \tau_i), \tag{8}$$

in which τ_i is the correlation time that describes the rapid internal motion.

The ^{31}P–^1H shift correlation spectrum was recorded at 4.7 T and 25° on a Bruker WM200 spectrometer over a spectral width of 800 Hz in F2 and 1800 Hz in F1, using 1024 points in F2 and 128 points in F1.

RESULTS AND DISCUSSION

Assignments of the ^1H resonances. — The ^1H resonances were assigned using a NOESY spectrum acquired with a mixing time of 300 ms, and a two-quantum-filtered COSY experiment (see Experimental). A portion of the 300 ms NOESY is shown in Fig. 1A, showing the sequential connectivities from the base proton resonances to the H-1′ resonances (left panel) and H-2′a/H-2′b resonances (right panel). Despite the significant overlap of some resonances, complete assignments were possible by using different routes of sequential connectivities, including most of the H-5′a, H-5′b resonances. The sugar resonances were checked using the COSY experiment, which gave essentially complete connectivities for H-1′, H-2′, H-3′, and H-4′ for most residues. Fig. 1B shows the H-1′–H-2′a/H-2′b and H-3′–H-2′a/H-2′b region of the COSY experiment. The coupling patterns will be discussed below. The assignments are given in Table I.

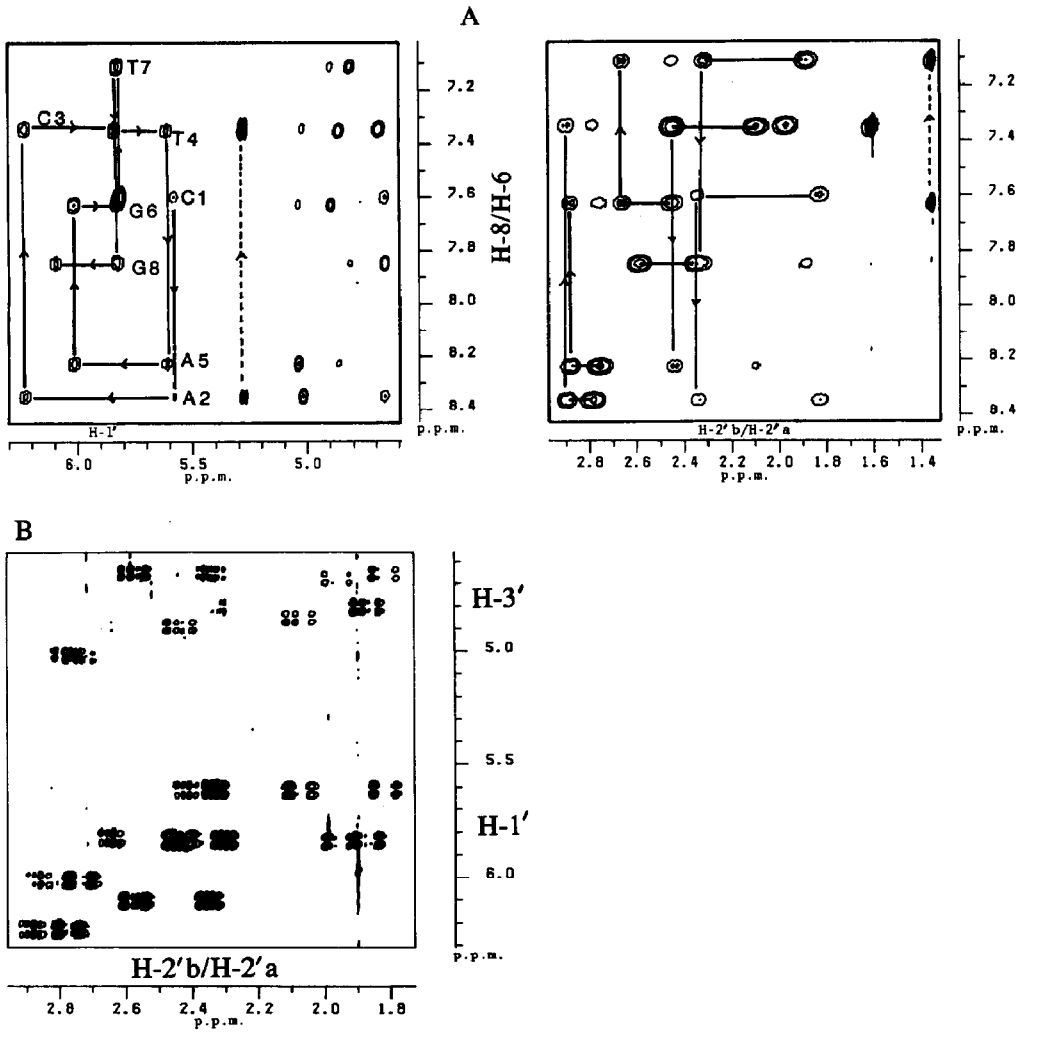

Fig. 1. ^{1}H-N-m.r. assignments of d(CACTAGTG)$_2$. A, NOESY spectrum recorded with a mixing time of 300 ms. The left panel shows the sequential n.O.e. connectivitics for the base proton via the H-1′ resonances and the right panel shows the base proton connectivities via the H-2′a/H-2′b resonances (the H-2a′,H-2′b resonances within the same sugar are connected by a horizontal line). B, 2-quantum-filtered COSY experiment; the region shows the coupling from the H-1′ resonances to the H-2′a and H-2′b resonances.

The central core of the molecule contains the sequence CTAG which is the most important in the trp operator for recognition by the trp repressor according to mutation studies[38] and the X-ray structure of the repressor-DNA complex[39]. This sequence has been studied by ^{1}H-n.m.r. spectroscopy when embedded in a 20 base-pair operator fragment[4]. The bases immediately 5′ and 3′ to the tetramer are the same in both molecules. Therefore, it is instructive to compare the chemical shifts of the proton resonances in the tetramer. Fig. 2 shows the differences in the chemical shifts ($\Delta\delta$) of

TABLE I

^{1}H-n.m.r. assignments[a] of d(CACTAGTG)$_2$ at 25°

Base	*H-8/H-6*	*H-5/H-2/Me*	*H-1'*	*H-2'a*	*H-2'b*	*H-3'*	*H-4'*	*H-5'a/ H-5'b*
Cyt1	7.61	5.82	5.58	1.84	2.35	4.67	4.03	3.7/3.71
Ade 2	8.37	7.82	6.23	2.78	2.90	5.02	4.42	4.15/4.25
Cyt 3	7.36	5.28	5.85	1.98	2.45	4.69	4.25	n.d.[b]
Thy 4	7.37	1.61	5.62	2.10	2.43	4.87	4.14	4.08
Ade 5	8.24	7.22	6.02	2.76	2.89	5.03	4.38	4.22
Gua 6	7.63	—	5.83	2.46	2.67	4.90	4.38	4.19/4.24
Thy 7	7.12	1.35	5.82	1.88	2.32	4.82	4.15	4.08/4.11
Gua 8	7.85	—	6.09	2.59	2.37	4.67	4.18	4.08

[a] Resonances were assigned from NOESY as described in the text. Chemical shifts (in p.p.m.) are referenced to internal DSS.[b] Not determined.

selected protons. While $\Delta\delta$ values of <0.05 p.p.m. are probably not significant, there are several $\Delta\delta$ values of >0.1 p.p.m., all of which involve sugar protons. The largest $\Delta\delta$ values are found for the first two residues in the CTAG subsequence (*i.e.*, C3 and T4 in the octamer). These $\Delta\delta$ values may reflect subtle conformational differences between the long and short fragments.

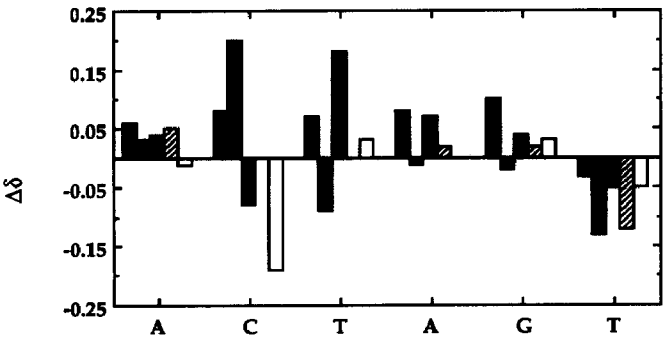

Fig. 2. $\Delta\delta$ Values for the ACTAGT segment in the octamer and in 20 base-pair oligonucleotides. Assignments for the 20 base-pair DNA fragments were taken from ref. 4 and averaged for the two sub-sequences as described in the text. Chemical shift differences are plotted as octamer values minus 20-mer values: ■, H-8/H-6; ■, H-1'; ■, H-2'a; ▨, H-2'b; □, H-3'.

Assignments of the ^{13}C resonances. — Fig. 3 shows a ^{13}C–^1H shift-correlation spectrum and a broad-band decoupled carbon spectrum. As the protons have been assigned, the resonances of the proton-bearing carbons can also be simply assigned. The C-2'–H-2'a/H-2'b of the A2 and A5 peaks are of very low intensity in the two-dimensional experiment, possibly due to the rapid relaxation of both the carbon and the protons. However, the resonances are visible in the broad-band decoupled one-dimen-

sional experiment, allowing them to be partly assigned by difference. Similarly, the cross-peaks for the A2C-2–A2C-2H and TC-6–TH-6 are not present in the two-dimensional experiment, and therefore could not be assigned. The chemical shift data are given in Table II.

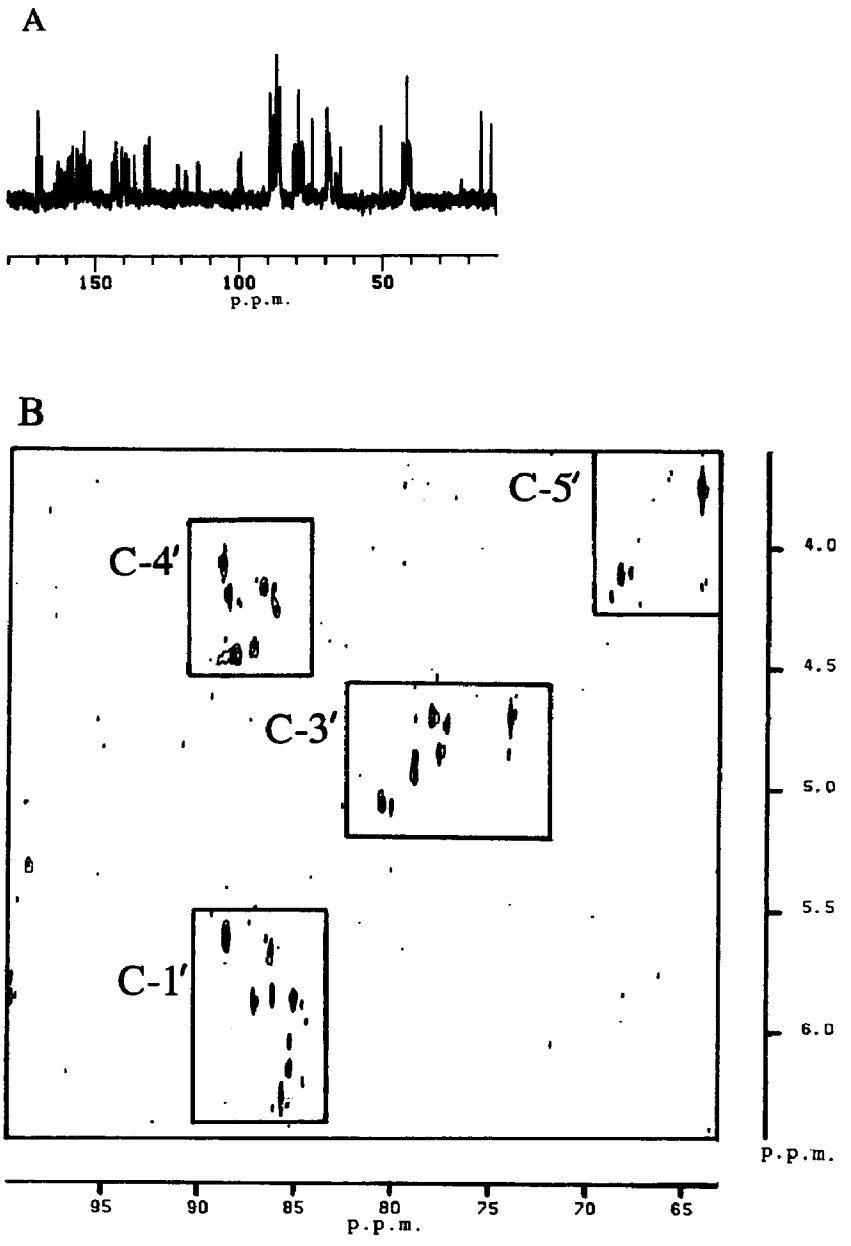

Fig. 3. ^{13}C-N.m.r. spectra of d(CACTAGTG)$_2$. A, One-dimensional spectrum (protons were decoupled using Waltz 16). B, Heteronuclear shift-correlation (the region containing the C-1′, C-3′, C-4′, and C-5′ resonances is shown).

TABLE II

^{13}C-n.m.r. assignments[a] at 25°

Base	*C-6/C-8*	*C-2/C-5/CMe*	*C-1'*	*C-2'*	*C-3'*	*C-4'*	*C-5'*
Cyt 1	143.5	99.6	88.5	41.0	77.9/73.9[b]	88.8	64.4
Ade 2	142.1	155.7	85.5	39.8/40.7	80.4	88.0	n.d.[d]
Cyt 3	142.6	98.7	87.1	40.0	77.2	85.9	n.d.
Thy 4	140.2	15.2	86.2	39.6	78.9	86.7	n.d.
Ade 5	142.2	n.d.	85.2	39.8/40.7	79.9	87.2	n.d.
Gua 6	n.d.	—	86.1/85.0[c]	41.6	78.8	87.2	n.d.
Thy 7	n.d.	14.8	85.0/86.1[c]	40.0	77.5	86.1	n.d.
Gua 8	139.4	—	85.2	42.4	73.9/77.9[b]	88.4	n.d.

[a] Resonances were assigned from the heteronuclear shift-correlated spectrum, using the proton assignments given in Table I. Chemical shifts (p.p.m.) are referenced to internal DSS. [b] Owing to the overlap of the H-3' resonances, these carbons are not individually assigned. [c] Owing to the overlap of the H-1' resonances, these carbons are not individually assigned. [d] Not determined.

Generally, the ^{13}C chemical shifts fall into groups as described by Leupin *et al.*[40], such that the C-1'–H-1', C-3'–H-3', and C-2'–H-2'a/H-2'b regions are completely resolved in the two-dimensional experiment. This separation allows the relaxation properties of individual CH vectors to be measured unambiguously (see below).

Assignments of the ^{31}P resonances. — Fig. 4A shows a one-dimensional ^{31}P-n.m.r. spectrum of the octamer recorded at 81 MHz. As only seven resonances are resolved, it appears that the two strands are magnetically equivalent, which is in agreement with the ^{1}H-n.m.r. spectra. The ^{31}P–^{1}H shift correlation spectrum is shown in Fig. 4B. The phosphorus resonances were assigned by correlation with the H-3' and H-4', H-5'a, H-5'b resonances. The assignments are given in Table III. The range of the chemical shifts is only 0.35 p.p.m., which is substantially less than that commonly observed for duplex DNA ($\Delta\delta \approx 0.5$ p.p.m.). However, as the lines are sharp, the individual resonances are resolved. Further, the 20 base-pair trp operator and mutants thereof show a dispersion of 0.61 p.p.m., whereas the hexamer d(CGTACG)$_2$ shows a dis-

TABLE III

^{31}P-N.m.r. assignments[a] of CACTAGTG at 25°

Phosphate	δ	*Phosphate*	δ
C1pA2	−17.27	A5pG6	−17.35
A2pC3	−17.51	G6pT7	−17.57
C3pT4	−17.34	T7pG8	−17.62
T4pA5	−17.44		

[a] ^{31}P resonances were assigned by heteronuclear shift-correlation, using the proton assignments given in Table I. Chemical shifts (p.p.m.) are referenced to external methylene diphosphonate at 0 p.p.m. (16.3 p.p.m. from 85% aqueous phosphoric acid).

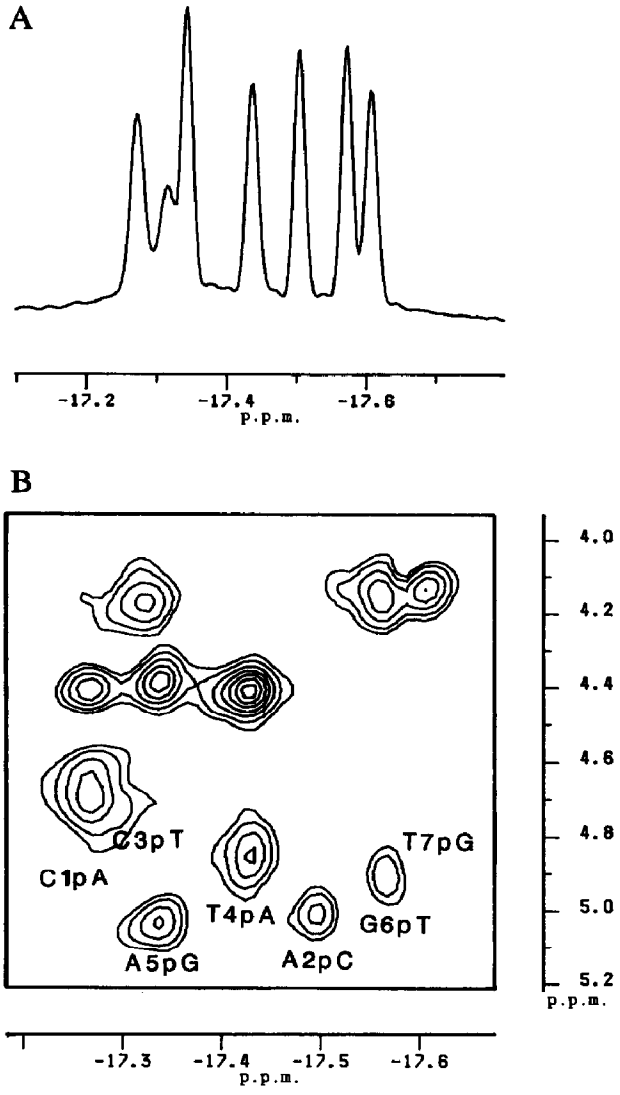

Fig. 4. ^{31}P-N.m.r. spectra of d(CACTAGTG)$_2$. A, One-dimensional spectrum resolution enhanced using the Lorentz-to-Gauss transformation (LB = −2.5, GB = 0.25). B, Shift-correlation spectrum; the free induction decays were zero-filled once in F2 and twice in F1, and multiplied by sine-squared functions shifted 36° in F2 and 60° in F1 prior to Fourier transformation.

persion of 0.55 p.p.m.[26]. Also, the chemical shifts in the octamer are in the low-field range found for other sequences. This finding may indicate a particular restricted range of backbone angles in the octamer compared with other B-like fragments of DNA[41].

Conformation. — (a) Puckering of the deoxyribose ring. Fig. 5A shows a resolution-enhanced region of the ^{1}H-n.m.r. spectrum in which the coupling between H-1′ and H-2′a,H-2′b can be clearly observed for three of the nucleotides. The splitting pattern is a double doublet for two of these H-1′ resonances, for which $\Sigma_{1'}$ = 14.8 Hz, and the

other is a triplet for which $\Sigma_{1'} = 14.3$ Hz. Although this splitting places the dominant conformation of these residues in the south domain, the coupling is incompatible with pure C-2'endo[20]. Either there is a mixture of conformations, or the pseudorotation angle is near 200° (*i.e.*, near C-3'exo). Further information was obtained from the 300-ms NOESY spectrum, in which H-1' to H-2'a and H-2'b cross-peaks are resolved, and sums of the coupling constants can be determined. Some cross-sections through the H-1'–H-2'a cross-peaks are shown in Fig. 5B. Because the fine structure of the NOESY cross-peaks is all in-phase, the sums of the coupling constants may be slightly underestimated. In contrast, the cross-peaks are in antiphase in the two-quantum-filtered COSY experiment, which tends to lead to an overestimation of the coupling constants[42]. By comparing the results of the two experiments, it is possible to estimate the errors from this source. The fine structure of the COSY cross-peaks is visible in Fig. 1B. The results of the independent determinations of the sums of coupling constants are compared in Table IV. In general, the sums of coupling constants determined from the COSY experiment are slightly larger than those determined from the NOESY experiment, although the agreement is quite good, given the digital resolution of 0.9 Hz per point. In addition, the sums of the coupling constants derived from the two-dimensional experiments agree well with those determined from one-dimensional experiments, where the comparison is possible.

The data in Table IV can be used to rule out areas of conformational space; for all nucleotides, the conformation must be mainly in the south domain. If a single conformation is assumed, the coupling constants are loosely compatible with conformations near C-3'exo for all sugars. However, the quantitative agreement with the coupling constants is poor. Better agreement can be obtained by analysing the conformation as a mixture of puckers with $P_N \approx 9°$. The conformational parameters P_s and f_s were

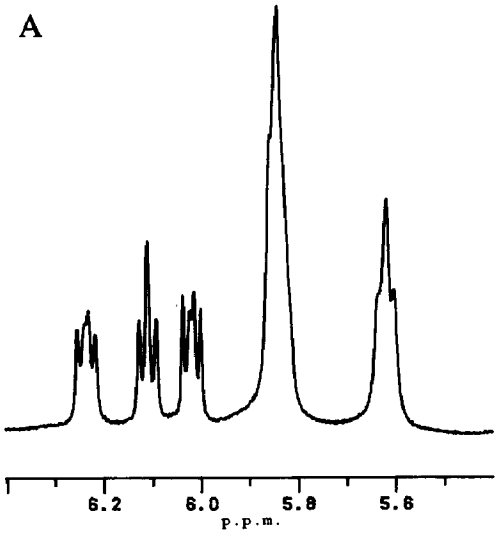

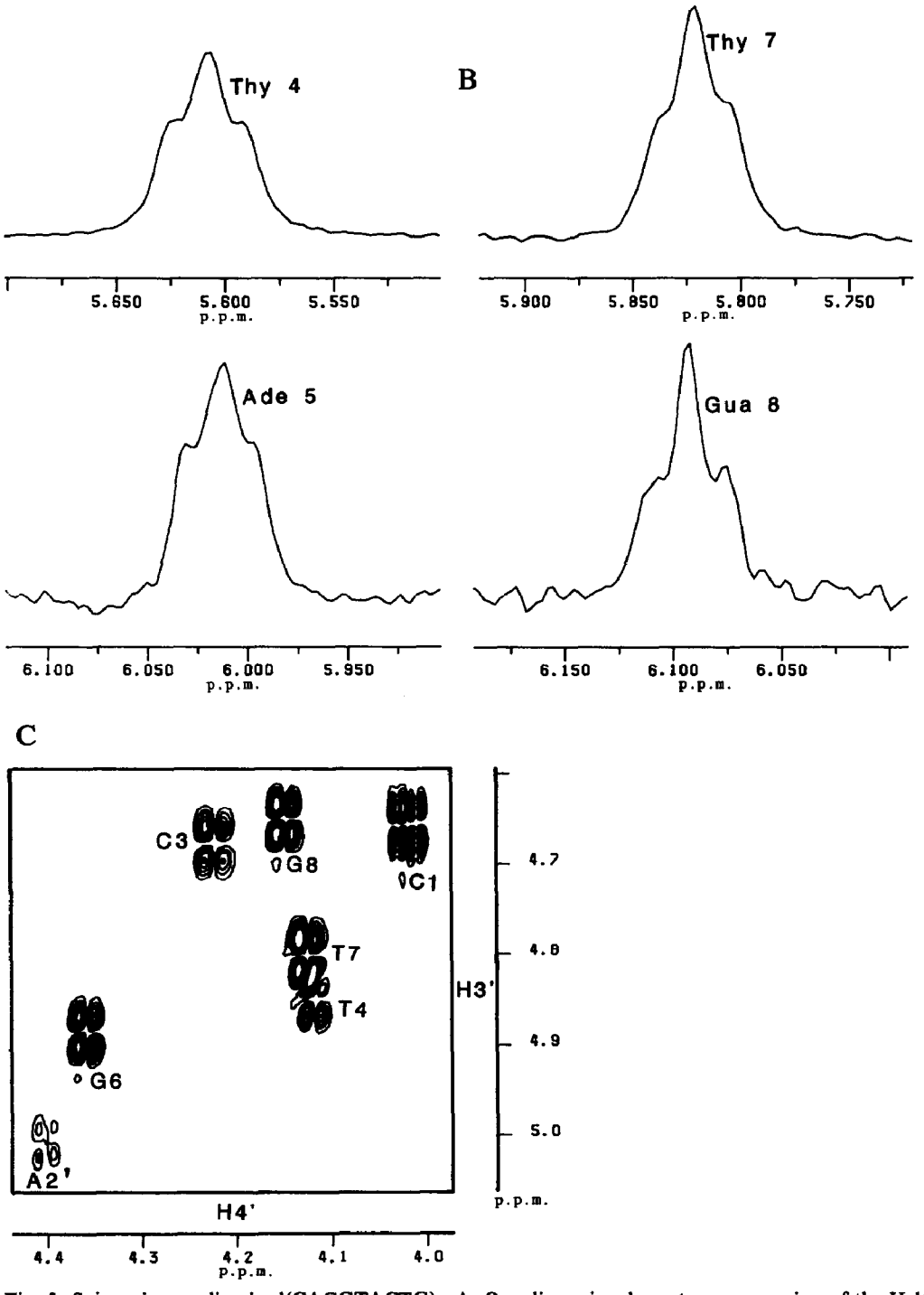

Fig. 5. Spin–spin coupling in d(CACGTACTG)$_2$. A, One-dimensional spectrum: expansion of the H-1′ region; the spectrum has been resolution enhanced using the Lorentz-to-Gauss transformation with LB = −2.5, GB = 0.25. B, Cross-sections from the NOESY spectrum recorded with a mixing time of 300 ms. C, Section of the 2-quantum-filtered COSY showing the H-3′–H-4′ cross-peaks.

TABLE IV

Sugar conformations[a]

Base	Σ_1'	$\Sigma_{2'a}$	$\Sigma_{2'b}$	f_s	P_s	*R.m.s.*	$r_{1',4'}$ (Å)		$J_{3',4'}$
	(Hz)	*(Hz)*	*(Hz)*		*(°)*		*Calc.*	*Obs.*	*(Hz)*
Cyt 1	13/14	n.d.[b]/28	n.d./21.5	0.75	182	0.32	3.0	3.25	2.8
Ade 2	14.8/15	27/27	n.d./23	0.88	200	0.41	3.6	3.15	1.9
Cyt 3	13.5/14.5	26/28	n.d./n.d.	0.8	177	0.1	3.15	2.9	2.6
Thy 4	14.2/15	27/28	n.d./23	0.89	196	0.45	3.4	3.1	1.8
Ade 5	14.8/15.5	26/26.5	n.d./n.d.	1.0	212	0.29	3.5	3.0	0.9
Gua 6	14.0/14.5	n.d./n.d.	22/22	0.84	178	0.1	3.2	3.1	2.3
Thy 7	n.d./14.5	26/n.d.	22/n.d.	0.87	190	0.57	3.4	n.d.	2.1
Gua 8	14.3/14.5	28/28	23/22	0.85	180	0.39	3.3	n.d.	2.2

[a] The first value for the coupling constants was determined from NOESY, and the second from 2-quantum-filtered COSY. Average errors on coupling constants: ± 1 Hz for $\Sigma_{1'}$, ± 1.5 Hz For $\Sigma_{2'a}$ and ± 2 Hz for $\Sigma_{2'b}$. f_s and P_s were calculated by least-squares fitting to sums of coupling constants, assuming a value for P_N of 9°, and $\phi_m = 37°$. The expected values of $J_{3',4'}$ were calculated for these sugar parameters, and the effective distance $r_{1',4'}$ was calculated assuming weighted averaging of the appropriate cross-relaxation rate constant. This slightly underestimates the effective distance (see text). [b] Not determined.

determined by least-squares analysis, with the pseudorotation amplitude factor fixed at 37° for both states. Good agreement with the data was obtained for all nucleotides, with r.m.s. agreements between the calculated and observed quantities of <0.5 Hz. With the exception of Cyt 1, all sugars appear to be $>80\%$ in the south state, and the best phase angles correspond to the range C-2'endo to C-3'exo. The remaining residues are consistent with fractions of the C-2'endo state observed in other systems[8–10,25,29]. However, given the imprecision of the experimental values, and the relatively weak dependence of the conformational parameters on the coupling constant, the values of P_s are determined to within only $\pm 20°$ at best, and f_s to $\sim \pm 0.1$. However, in support of the values given in Table IV, the only H-2'b–H-3' cross-peaks that show any intensity in the COSY experiment are those of C1/G8 and T7 (Fig. 1B). This cross-peak is present only if the relevant coupling constant is >2 to 3 Hz, which occurs only when an appreciable fraction of the C-3'endo state is present. Further, the H-3'–H-4' COSY cross-peak intensities are relatively strong (Fig. 5C), which is not expected for pure conformational states with $P > 162°$ (when $J_{3'4'}$ is <1 Hz). Using the conformational parameters found by least squares, the predicted values of $J_{3'4'}$ are also given in Table IV. With the exception of A5, the predicted coupling constant is >2 Hz, which will give rise to appreciable cross-peak intensity because both H-3' and H-4' are relatively narrow. The only H-3'–H-4' cross-peak that is missing (Fig. 5C) is that of A5, which is consistent with the calculations.

The n.O.e. for the H-1'–H-4' vector is sensitive to the pseudorotation angle, and reaches a maximum near $P = 90°$[21]. The intensity is similar for the C-3'endo and C-2'endo states. Further, as the distance exceeds 3.5 Å for $P > 198°$, the n.O.e. becomes very small for conformations in this range. Hence, this n.O.e. is significant only when the

sugars spend some of the time near O-4'endo ($P = 90°$). The apparent H-1'–H-4' distances were determined from n.O.e. time-courses on irradiation of H-1'. The correlation time was taken to be the same as that of the cytosine H-6–H-5 vectors, *i.e.*, 3.0 ns (see below). This n.O.e. is not significantly affected by spin diffusion, as there are no spins lying between H-1' and H-4'; this conclusion is supported by extensive simulations on oligomeric DNA (calculations not shown). Additional calculations using the formalism of Tropp[25,43] show that motions that affect the H-1'–H-2'b vector will have a similar effect on the H-1'–H-4' vector. The effect of internal motions on the H-1'–H-2'b vectors is small (see below). Such motions will tend to cause the distance to be slightly overestimated (by $<5\%$). Usually, the experimental distance is smaller than that expected for the C-3'exo state. However, given the difficulty in determining distances accurately, and also the errors in calculating distances within sugar rings as a function of phase angle, these discrepancies are small. Nevertheless, as the sugars do experience internal motions (see below), and the potential function for repuckering has rather broad minima[18,19], it is likely that the sugars are constantly fluctuating about a fairly wide range of angles. This view is supported by molecular dynamics calculations, which indicate fluctuations of 40° or more on the ps time-scale[9]. These fluctuations will have a relatively small influence on the coupling constants in the ranges of conformations found here[20,21]. The small observed values of $r_{1'4'}$ can be obtained if states near O-4'endo are sampled on average only 20–25% of the time.

Thus, although a fairly simple description of the conformation of the sugars can be found that accounts for the data, the overall precision is relatively low, and a simple two-state equilibrium seems intrinsically oversimplified. This conclusion is the same as that reached by Gochin *et al.*[9,10], using similar kinds of data. Fortunately, the imprecision in the determination of the sugar conformation has little influence on the determination of the glycosidic torsion angles[5,16] (and see below).

(*b*) *Glycosidic torsion angles.* One-dimensional n.O.e. time courses were determined on irradiation of H-8 or H-6 of each nucleotide, and observing the n.O.e. to the H-1', H-2'a, H-2'b, and H-3' resonances, using irradiation times of 50, 100, 200, 300, and 500 ms. The glycosidic torsion angles were determined, using the program NUCFIT[16], by optimising both the glycosidic torsion angle and the pseudorotation phase angle or the fraction south, and the spin–lattice relaxation rate constants as described[5,44]. Fig. 6 shows typical fits to the data for Gua 6 and Thy 7. Because 15–20 data points are used to define only two conformational parameters, the conformation is well described, particularly the glycosidic torsion angle. The best fit parameters are given in Table V. As can be seen, the glycosidic torsion angles are well determined (errors $<\pm 2°$). If the pseudorotation phase angle is allowed to vary, equally good fits can be achieved in an interval of $126 < P_s < 198°$. Similarly, the value of f_s is determined only to within ± 0.1 by the n.O.e. data. The best fit values given in Table V were obtained by holding P_s to the value found from the coupling constant analysis (Table IV), and systematically searching and optimising the glycosidic torsion angles and f_s. As Table V shows, the best description of the sugar conformations is generally high anti, in which the glycosidic torsion angles for the pyrimidines are larger than those for the purines. The agreement

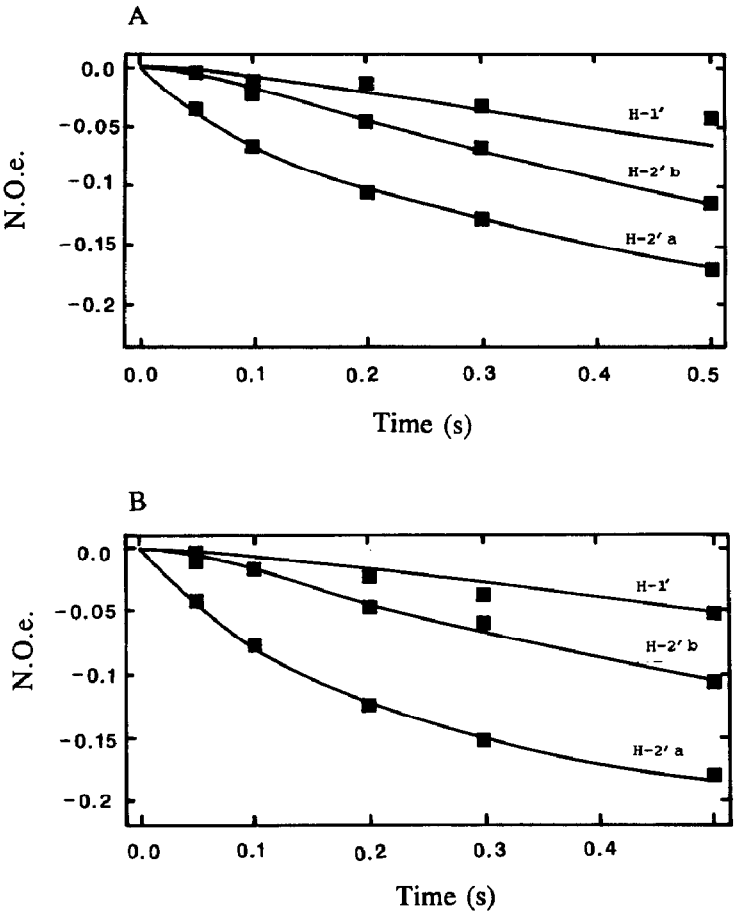

Fig. 6. The conformation of the nucleotide units: A, N.O.e.'s for Gua 6 on saturation of the H-8 resonance; B, N.O.e.'s for Thy 7 on saturation of the H-6 resonance.

between f_s determined from coupling constants and the n.O.e. data is generally within experimental error.

It is instructive to compare the glycosidic torsion angles for the CTAG segment in the octamer with those determined for the same sequence within the 20 base-pair fragment of the trp operator. As the 20-mer contains two copies of the CTAG subsequence[4,5], the glycosidic torsion angles for the 20-mer have been averaged. The absolute values of the glycosidic torsion angles differ by $<5°$ (r.m.s. difference = 3.9°), and the trends along the sequence are very similar (Fig. 7). The angles for the purines are $-104 \pm 4°$ and $-118 \pm 5°$ for the pyrimidines. This difference of about 10° on average has been noted previously in other sequences[5,11,44], and appears to be a property of purines versus pyrimidines, at least within the B-family of conformations. It seems also that the $\Delta\delta$ values between the molecules (see above) arise from differences in the relative orientations of neighbouring base pairs, rather than in the conformations of individual

TABLE V

Nucleoside conformations from n.O.e. intensities[a]

Base	*X*	f_s	R	*Base*	*X*	f_s	R
Cyt 1	−128	0.91	0.10	Thy 4*[b]	−113	0.91	0.10
Cyt 1*	−124	0.71	0.12	Ade 5	−102	0.95	0.14
Ade 2	−100	0.93	0.10	Gua 6	−110	0.93	0.06
Cyt 3	−116	(0.8)	0.03	Gua 6*	−108	0.88	0.07
Thy 4	−114	0.99	0.12	Thy 7	−117	0.95	0.09

[a] Pseudorotation phase angles were taken from Table IV, and the fraction of the C-2'endo state was optimised with the glycosidic torsion angle, using NUCFIT. [b]* The value of the glycosidic torsion angle for the nucleotide in the C-3'endo state was held at −155°. For Cyt 3, only the H-6–H-2' data were available, so f_s was held fixed at 0.8 for this residue.

nucleotide units. The conformation of the CTAG segment, at least at the level of the nucleotide units, is essentially the same in both the octamer and the 20 base-pair fragments, in which the sugars are largely in the south domain, and the glycosidic torsion angles are near to −110°. This conclusion is at variance with an X-ray crystal structure[45] of d(CTCTAGAG)$_2$, in which the sugars' puckers were near C-3'endo, and the glycosidic torsion angles were near to −160°, *i.e.*, values typical of the A-family of structures. The intranucleotide n.O.e.'s observed for the present related octamer are inconsistent with the A-structure, which would require rather small H-2'a–H-8/6 n.O.e.'s[16]. It is evident that there are substantial differences between the crystal and solution states for this sequence, as has been observed for other DNA fragments[46]. However, although the n.O.e. data and the coupling constants imply that the nucleotide conformations are similar to those in B-DNA, the ^{31}P chemical shifts suggest that the backbone conformation may differ somewhat from that expected for canonical B-DNA (see above). A detailed analysis of the helical structure of the octamer will require additional data.

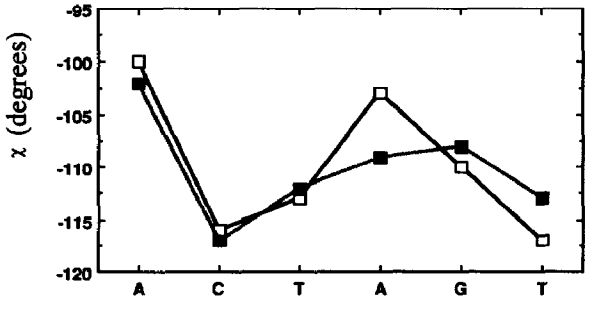

Fig. 7. Comparison of the glycosidic torsion angles in the octamer and in the 20 base-pair trp operator; the glycosidic torsion angles for the 20-mer were taken from ref. 5: □, octamer; ■, 20-mer.

Dynamics. — An octamer of B-DNA is expected to have dimensions of approximately 27 Å by 23 Å, which, for the purposes of overall rotation, can be considered as being isotropic. A lower limit to the rotational correlation time was obtained by measuring the cross-relaxation rate constant for the two cytosine H-6–H-5 vectors[34]. The measured values, determined from n.O.e. time courses, were -0.75 ± 0.1 s^{-1}, which translates to a correlation time of 3.0 ± 0.4 ns, assuming a proton–proton distance of 2.46 Å. This value is slightly higher than expected based on the behaviour of 6, 12, 14, and 20 base-pair fragments[47], but lies within the experimental error. It is possible that, at the higher nucleotide concentrations used in this study (6.5mM strands), the viscosity is higher than that of pure D_2O.

Internal motions of the H-1′–H-2′b, H-2′a–H-2′b, and H-2′a–H-3′ sugar vectors, where resolution permitted, were determined from n.O.e. time courses, using the program FITSIG[25]. In general, the cross-relaxation rate constants for the H-1′–H-2′b vectors are well determined. Only two H-2′a–H-2′b cross-relaxation rate constants were determined directly by irradiation of the only well-resolved H-2′ peaks; the remainder were determined indirectly from the cross-relaxation pathway H-1′–H-2′b–H-2′a obtained by saturating H-1′ and observing the n.O.e. to H-2′b and H-2′a. The cross-relaxation rate constant for H-2′a–H-2′b is less well determined under these conditions, as the results in Table VI show. Most of the apparent order parameters for the H-1′–H-2′b vectors are between 0.7 and 0.8, which are very similar to those values obtained from a similar study of a hexamer[25]. The H-2′a–H-2′b vectors are of similar magnitude, or possibly slightly larger, which is again consistent with the previous results on the hexamer. As Reid *et al.*[23] have pointed out, small errors in the estimation of proton–proton distances can have a significant influence on derived correlation times; an error of only 1.5% (*i.e.*, 0.035 Å at 2.3 Å) leads to an error of 9% in the cross-relaxation rate constant. Hence, the order parameters, which are calculated as a ratio of the cross-relaxation rate constants, may have an intrinsic uncertainty of ~20% from this consideration alone. Nevertheless, the measured cross-relaxation rate constants are all lower than expected for a correlation time of 3 ns, which is supported by the ^{13}C relaxation data described below. The poor agreement with the sugar conformational equilibria and the ranking of the apparent order parameters suggests that motions other than pseudorotation are occurring (the apparent order parameters are upper estimates, as the cytosine H-6–H-5 vectors give a lower limit to the overall tumbling time of the molecule). For example, both Thy 4 and Ade 5 show a high degree of conformational purity according to both scalar and dipolar coupling data (*cf.* Tables IV and V), yet the apparent order parameters for the H-1′–H-2′b and H-2′a–H-2′b vectors are less than unity. Taking the apparent order parameters at face value, and assuming rapid motion within a cone, the semi-angle of the cone can be calculated (according to ref. 36) from:

$$S^2 = 0.25 \cos^2\phi\,(1 + \cos\phi)^2. \qquad (9)$$

For order parameters in the range 0.7–0.8, the value of ϕ is 22–28°. This range of angles is similar to that reported[24] for the C-2′–D vectors of the adenine residues in the

hydrated dodecamer d(CGCGAATTCGCG)$_2$. It is also clear that it is unnecessary to invoke radically different correlation times for proton–proton vectors in the sugars versus those in the bases.

TABLE VI

Sugar mobility determined from proton-proton cross-relaxation rates[a]

Vector		σ (s^{-1})	S^2(*app*)
Cyt 1	H-1′–H-2′b	−0.55	0.5
	H-2′a–H-2′b*	−4.66	0.9
Ade 2	H-1′–H-2′b	−0.86	0.75
	H-2′a–H-2′b*	−4.2	0.81
Cyt 3	H-2′a–H-2′b	−3.25	0.63
	H-2′a–H-3′	−0.8	0.7
Thy 4	H-1′–H-2′b	−0.86	0.75
	H-2′a–H-2′b	−3.7	0.71
	H-2a′–H-2′b*	−4.2	0.81
	H-2′a–H-3′	−0.8	0.7
Ade 5	H-1′–H-2′b	−0.91	0.79
	H-2′a–H-2′b*	−4.3	0.83
Gua 6	H-1′–H-2′b	−0.81	0.70
Thy 7	H-1′–H-2′b	−1.1	0.95
	H-2′a–H-2′b*	−4.5	0.87

[a] S^2(app) is the apparent order parameter defined as the ratio of the observed cross-relaxation rate constant to that calculated assuming a correlation time equal to that of the Cyt H-6–H-5 vector (*i.e.*, 3 ns). The estimated error on the cross-relaxation rate constants is ±10% except those marked*, where the error is ±25%.

The steady-state n.O.e. and ^{13}C spin–lattice relaxation rate constants for the assigned CH vectors were determined as described in the Experimental. Fig. 8 shows the C-3′ region with and without n.O.e. and a typical R_1 recovery curve with the non-linear regression line. Clearly several of the C-3′ resonances show a substantial n.O.e. (*i.e.* > 1.2). The experimental n.O.e. and R_1 values are given in Table VII. As the spectra were fairly noisy, these relaxation parameters are subject to a considerably higher error than those determined by ^1H-n.m.r. For an overall tumbling time of 3 ns, the $\{^1H\}$–^{13}C n.O.e. is expected to be at the minimum value of 1.16, the value $R_1/n = 3.5\,s^{-1}$, and a linewidth of ~4 Hz in the absence of internal motion. All the protonated carbon atoms of the bases showed small (1.15 ±0.1) n.O.e.'s and R_1 values of 3.2 ±0.2 s^{-1}, except for the thymidine methyl carbons, for which the values of R_1/n were 1.4 s^{-1}. This finding is consistent with substantial motion, as expected for a methyl group. Hence, the relaxation properties of the bases can be adequately described using the rigid body formulation, which implies that any librations occurring in the sub-ns time range have small

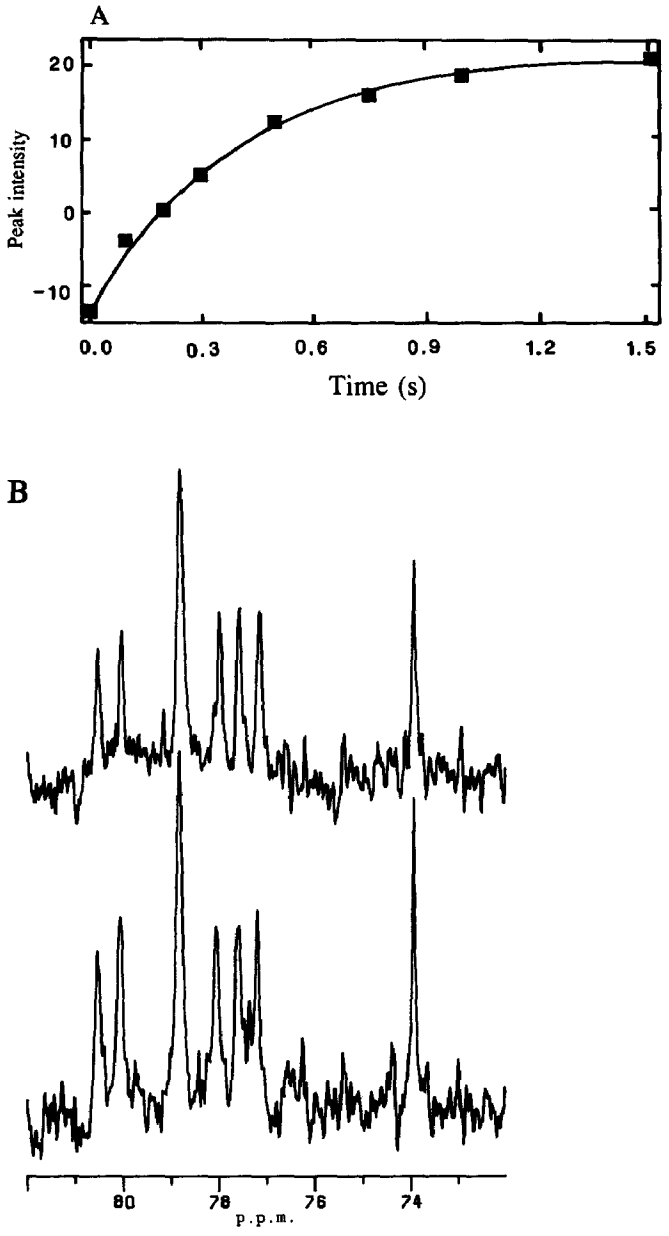

Fig. 8. ^{13}C Relaxation in the octamer: A, inversion recovery curve for Thy 4 C-1′; B, proton-decoupled spectra showing the C-3′ region with (lower) n.O.e. and without (upper) n.O.e.

TABLE VII

^{13}C Relaxation properties of assigned resonances[a]

Carbon		*N.O.e.*	R_1/n (s^{-1})	S^2	τ_i (*ns*)
Cyt 1	C-6	1.1	3.0	>0.9	—
	C-5	1.1	2.8	>0.85	—
	C-2′	1.47	1.7	0.5	0.07
	C-3′	1.8	2.0	0.4	0.06
	C-4′	1.60	2.0	0.47	0.05
	C-5′	1.76	2.1	0.44	0.06
Ade 2	C-8	1.1	3.3	1.0	—
	C-2	1.1	3.2	1.0	—
	C-3′	1.59	2.8	0.8	0.08
Cyt 3	C-6	1.1	3.0	>0.9	—
	C-5	1.1	3.4	1.0	—
	C-2′	1.25	1.9	0.58	<0.05
	C-3′	1.27	2.2	0.67	<0.1
Thy 4	C-6	1.14	3.9	1	—
	Me	1.3[b]	1.4	—	—
	C-2′	1.14	2.3	0.7	0.1
	C-3′	1.23	2.6	0.79	0.01
Ade 5	C-8	1.14	3.3	1.0	—
	C-2′[c]	1.1	1.8	0.5	0.12
	C-3′	1.57	2.6	0.76	<0.05
	C-4′	1.34	2.7	0.8	<0.1
Gua 6	C-2′	1.10	2.3	0.7	<0.1
	C-3′	1.2	2.6	0.79	<0.05
Thy 7	Me	1.3[b]	1.4	—	—
	C-3′	1.23	2.1	0.65	<0.05
Gua 8	C-8	1.15	3.1	>0.9	—
	C-1′	1.1	2.7	0.8	<0.1
	C-2′	1.3	1.4	0.42	<0.05
	C-3′	1.2	2.0	0.6	<0.1
δ 87.4	C-4′	1.34			

[a] Relaxation parameters were determined as described in the text. The statistical error on R_1 is 15%. τ_i is the correlation time of the internal motion. The error on S^2 is $\sim \pm 0.1$, and on $\tau_i \sim 50\%$. [b] Value underestimated owing to partial saturation in the n.O.e. experiment. [c] Resonance at 39.8 p.p.m.

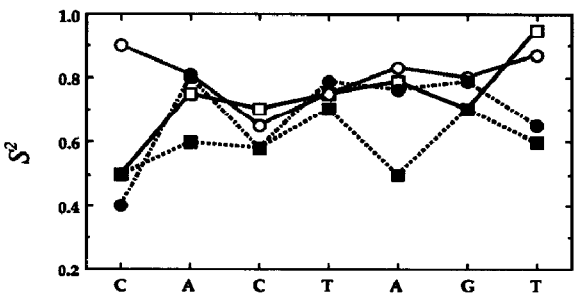

Fig. 9. Variation of the apparent order parameters along the sequence (the order parameters were taken from Tables VI and VII): □, H-1′–H-2′b; ○, H-2′a–H-2′b; ■, C-2′–H; ●, C3′–H.

amplitudes. The same is not true for the sugar carbons. For the terminal residues, Cyt 1 and Gua 8, many of the sugar CH vectors show substantial n.O.e.'s, and R_1 values approximately two-fold smaller than those obtained for the bases. This is clear evidence for substantial internal motions for the terminal bases, in agreement with the proton data for Cyt 1 (see above). However, C-2′ and C-3′ of the internal residues also show larger n.O.e.'s and smaller R_1 values than in the bases, indicating the presence of significant rapid internal motions. The mobility can be characterised by two parameters, the order parameter S^2 which characterises the spatial extent of the motion, and a correlation time τ_i which characterises the timescale of the motion[36]. The data in Table VII have been fitted by least-squares analysis to Eq. *6–8*. However, as the data are noisy, and the form of the function is not very sensitive to the value of τ_i, this latter parameter is very poorly determined, and equally good fits could be obtained in the range τ_i = 0–0.1 ns. Nevertheless, the apparent order parameters for the C-2′ and C-3′ CH vectors are small at the termini, and larger in the centre of the molecule. The average order parameters for non-terminal residues are S^2 = 0.62 for C-2′ and 0.74 for C-3′; these values are equivalent to motion of the vectors in cone angles of 25° and 32°, respectively. The CH order parameters follow the trends observed for the HH vectors (Fig. 9), and are of similar magnitude. However, the amplitudes of the motion(s) are fairly small, and are similar to what would be expected for thermal fluctuations on the 1–100 ps time-scale. Fluctuations of this size have only modest effects on proton n.O.e.'s, and will have little influence on the determination of the conformation of oligonucleotides using n.m.r. data.

CONCLUSIONS

The nucleotide units of the octamer $d(CACTAGTG)_2$ are all in conformations typical of B-DNA in solution, in contrast to the crystal state[45]. However, details of the backbone, which are not revealed by the present study, may be significantly different from the classical B conformation, a hint of which is provided by the chemical shift dispersion of the ^{31}P resonances. The difference of 10° in the glycosidic torsion angles between purine and pyrimidine nucleotides may be explained partly by the nature of the glycosidic linkage. In the former, the sugar is attached to a five-membered ring, whereas in the latter it is attached to a six-membered ring, resulting in a distance between H-6 and H-2′a ~0.3 Å shorter than that between H-8 and H-2′a. For angles $< -110°$, the distance between H-6 and H-2′a becomes less than the sum of the van der Waals radii, whereas van der Waals violations occur at angles $< -100°$ for H-8–H-2′a.

Both ^1H and ^{13}C relaxation data indicate that there are internal motions, occurring on the sub-ns time-scale, that affect the sugars more than the bases, with the greatest influence on the terminal residues. The motions affecting the central sugars can be thought of as a libration with an amplitude of around 20°. These motions should be accessible to molecular dynamics simulations. They are also comparable to amplitudes estimated by deuterium relaxation in a dodecamer[24] and by ^{13}C relaxation in polynucleotides[37,48].

ACKNOWLEDGMENTS

This work was supported by the Medical Research Council. I thank Brian Peck for the purification of the oligonucleotide, and Dr. J. Feeney for helpful comments.

REFERENCES

1 M. Nilges, G. M. Clore, A. M. Gronenborn, N. Piet, A. Brünger, M. Karplus, and L. Nilsson, *Biochemistry*, 26 (1987) 3718–3733.
2 M. Nilges, G. M. Clore, A. M. Gronenborn, N. Piet, A. Brünger, and L. W. McLaughlin, *Biochemistry*, 26 (1987) 3734–3744.
3 N. Zhou, S. Managoran, G. Zon, and T. L. James, *Biochemistry*, 27 (1988) 6013–6020.
4 J.-F. Lefèvre, A. N. Lane, and O. Jardetzky, *Biochemistry*, 26 (1987) 5076–5090.
5 A. N. Lane, *Biochem. J.*, 273 (1991) 383–391.
6 W. Nerdal, D. R. Hare, and B. R. Reid, *Biochemistry*, 28 (1989) 10008–10021.
7 D. J. Patel, L. Shapiro, and D. R. Hare, *Q. Rev. Biophys.*, 20 (1987) 1–34.
8 L. J. Rinkel, G. A. van der Marel, J. H. van Boom, and C. Altona, *Eur. J. Biochem.*, 186 (1987) 87–101.
9 M. Gochin, G. Zon, and T. L. James, *Biochemistry*, 29 (1990) 11161–11171.
10 M. Gochin and T. L. James, *Biochemistry*, 29 (1990) 11172–11180.
11 A. N. Lane, T. C. Jenkins, T. Brown, and S. Neidle, *Biochemistry*, 30 (1991) 1372–1385.
12 E. P. Nikonowicz, R. P. Meadows, and D. G. Gorenstein, *Biochemistry*, 29 (1990) 4193–4204.
13 J. W. Keepers and T. L. James, *J. Magn. Reson.*, (1984) 404–426.
14 O. Jardetzky, *Biochim. Biophys. Acta*, 612 (1980) 227–232.
15 E. T. Olejniczak, C. M. Dobson, M. Karplus, and R. M. Levy, *J. Am. Chem. Soc.*, 106 (1984) 1923–1930.
16 A. N. Lane, *Biochim. Biophys. Acta*, 1049 (1990) 189–204.
17 A. N. Lane, *J. Magn. Reson.*, 78 (1988) 425–439.
18 W. K. Olson, *J. Am. Chem. Soc.*, 104 (1982) 278–286.
19 L. Nilsson and M. Karplus, *J. Comput. Chem.*, 7 (1986) 591–616.
20 L. J. Rinkel and C. Altona, *J. Biomolec. Str.*, 4 (1987) 621–649.
21 F. J. M. van de Ven and C. Hilbers, *Eur. J. Biochem.*, 178 (1988) 1–38.
22 R. Grütter, G. Otting, K. Wüthrich, and W. Leupin, *Eur. Biophys. J.*, 16 (1989) 279–286.
23 B. R. Reid, K. Banks, P. Flynn, and W. Nerdal, *Biochemistry*, 28 (1989) 10001–10007.
24 W.-C. Huang, J. Orban, A. Kintanar, B. R. Reid, and G. P. Drobny, *J. Am. Chem. Soc.*, 112 (1990) 9059–9068.
25 A. N. Lane and M. J. Forster, *Eur. Biophys. J.*, 17 (1989) 221–232.
26 M. J. Forster and A. N. Lane, *Eur. Biophys. J.*, 18 (1990) 347–355.
27 W. Eimer, J. R. Williamson, S. G. Boxer, and R. Pecora, *Biochemistry*, 29 (1990) 799–81.
28 J. A. McCammon and S. C. Harvey, in *Dynamics of proteins and nucleic acids*, Cambridge University Press, 1987, Chap. 6.
29 H. C. M. Nelson, J. T. Finch, F. L. Bonaventura, and A. Klug, *Nature, (London)*, 330 (1987) 221–226.
30 A. Bax and L. Lerner, *J. Magn. Reson.*, 79 (1988) 429–438.
31 G. Wagner and K. Wüthrich, *J. Magn. Reson.*, 33 (1979) 675–680.
32 D. Marion and K. Wüthrich, *Biochem. Biophys. Res. Commun.*, 124 (1983) 774–783.
33 T. A. Frenkiel, C. J. Bauer, M. D. Carr, B. B. Birdsall, and J. Feeney, *J. Magn. Reson.*, 90 (1990) 420–425.
34 A. N. Lane, J.-F. Lefèvre, and O. Jardetzky, *J. Magn. Reson.*, 66 (1986) 201–218.
35 R. K. Gupta, J. A. Ferretti, E. D. Becker, and G. H. Weiss, *J. Magn. Reson.*, (1980) 447–452.
36 G. Lipari and A. Szabo, *J. Am. Chem. Soc.*, 104 (1981) 4546–4558.
37 G. Lipari and A. Szabo, *Biochemistry*, 20 (1981) 6250–6256.
38 S. Bass, V. Sorrels, and D. Youderian, *Science*, 242 (1988) 240–245.
39 Z. Otwinowski, R. L. Schevitz, R.-g. Zhang, C. L. Lawson, A. Joachimiak, R. Q. Marmorstein, B. F. Luisi, and P. B. Sigler, *Nature (London)*, 335 (1988) 321–329.
40 W. Leupin, G. Wagner, W. A. Denny, and K. Wüthrich, *Nucl. Acids Res.*, 15 (1987) 267–275.
41 D. G. Gorenstein, S. A. Schroeder, J. M. Fu, J. T. Metz, V. Roongta, and C. R. Jones, *Biochemistry*, 27 (1988) 7223–7237.
42 D. G. Neuhaus, G. Wagner, M. Vasak, J. H. R. Kägi, and K. Wüthrich, *Eur. J. Biochem.*, 151 (1985) 257–273.

43 J. Tropp, *J. Chem. Phys.*, 72 (1980) 6035–6043.
44 A. N. Lane, *Biochim. Biophys. Acta*, 1049 (1990) 205–212.
45 W. N. Hunter, B. L. D'Estaintot, and O. Kennard, *Biochemistry*, 28 (1989) 2444–2451.
46 G. R. Clark, D. G. Brown, M. R. Sanderson, T. Chwalinski, S. Neidle, J. M. Veal, R. L. Jones, W. D. Wilson, G. Zon, and D. I. Stuart, *Nucl. Acids. Res.*, 18 (1990) 5521–5528.
47 A. J. Birchall and A. N. Lane, *Eur. Biophys. J.*, 19 (1990) 73–78.
48 M. E. Hogan and O. Jardetzky, *Biochemistry*, 19 (1980) 3460–3468.